Tolj, I. et al. (2013). Fuel cell-battery hybrid powered light electric vehicle (golf cart): Influence of fuel cell on the driving performance.
International Journal of Hydrogen Energy, 38: 10630 – 10639.
http://dx.doi.org/10.1016/j.ijhydene.2013.06.072

Fuel cell-battery hybrid powered light electric vehicle (golf cart): Influence of fuel cell on the driving performance

Ivan Tolj, Mykhaylo V. Lototskyy, Moegamat Wafeeq Davids, Sivakumar Pasupathi, Gerhard Swart and Bruno G. Pollet

Abstract

A light electric vehicle (golf cart, 5 kW nominal motor power) was integrated with a commercial 1.2 kW PEM fuel cell system, and fuelled by compressed hydrogen (two composite cylinders, 6.8 L/300 bar each). Comparative driving tests in the battery and hybrid (battery þ fuel cell) powering modes were performed. The introduction of the fuel cell was shown to result in extending the driving range by 63-110%, when the amount of the stored H_2 fuel varied within 55-100% of the maximum capacity. The operation in the hybrid mode resulted in more stable driving performances, as well as in the increase of the total energy both withdrawn by the vehicle and returned to the vehicle battery during the driving. Statistical analysis of the power patterns taken during the driving in the battery and hybrid-powering modes showed that the latter provided stable operation in a wider power range, including higher frequency and higher average values of the peak power.

1. Introduction

The use of proton exchange membrane fuel cells (PEMFC) in transportation has recently attracted great interest worldwide due to the fact that this type of fuel cell has a number of attractive properties, including positive environmental impact (the only by-products are pure water and heat), high efficiency, low operating temperature, high power density, fast start-up and response to load changes, simplicity, long life, etc. PEMFCs have been successfully demonstrated in various applications such as automobiles, scooters, bicycles, utility vehicles, distributed power generation, backup power, portable power, airplanes, boats and underwater vehicles [1].

There are many publications dealing with fuel cell-battery hybrid powered vehicles and systems. A recent review paper by Pollet et al. [2] highlighted the current status of hybrid, battery and fuel cell electric vehicles from electrochemical and market points of view. The paper analyses the existent engineering solutions, including architectures of hybrid electric drive trains. Cost, durability and energy

density are shown to be the main areas where improvements are required to compete with conventional fossil fuels. Some details relevant to the scope of the present study are outlined below.

Hwang and Chang [3] developed a hybrid powered light electric vehicle (LEV) in which the power system consisted of a PEMFC (the major propulsion power) and a lithium-ion battery pack (to provide peak power and to allow regenerative breaking). Barreras et al. [4] designed and developed a multipurpose utility AWDelectric vehicle (two 2.5 kW DC motors) with a hybrid power train based on a PEMFC and batteries. In this design, the vehicle reached a maximum speed of 11 km/h on a flat surface with a maximum power consumption of around 3 kW.

The development of a hybrid PEMFC and its integration into a mini-train is described by Hsiao et al. [5]. The power system is composed of a 200 W PEM fuel cell, four metal hydride (MH) hydrogen storage tanks operating at low pressure, a lead-acid battery pack, and an electronic energy control system. In this configuration, the fuel cell and lead-acid batteries were connected in parallel.

Jiang et al. [6] presented an experimental study on control strategies for active power sharing in a hybrid fuel cell-battery power source. Experimental tests were conducted with three control objectives: maximum power, maximum fuel cell efficiency, and adaptive strategy aimed to maintain a relatively constant battery voltage, by switching between the first two strategies.

Fisher et al. [7] integrated a lithium-ion battery pack, together with its management system, into a hydrogen fuel cell drive train in a lightweight city car. Electronic units were designed to link the drive train components and to allow system start-up, motor control and torque monitoring. The authors concluded that the electronic integration was successful, but the design needed optimisation and fine tuning. Thounthong et al. [8] proposed an energy system with a 500 W, 50 A PEMFC as a main power source, and battery (68 Ah, 24 V) with supercapacitor (292 F, 30 V, 500 A) as Electro-chemical Storage Devices. During starts/stops or other significant variations in load, the storage elements provided the balance of energy during the load transition period, and also absorbed excess energy from regenerative braking.

The development of a fuel cell system and its integration into a lightweight vehicle was presented by Hwang et al. [9]. The fuel cell system consisted of a 3.2 kW PEMFC, a micro-controller and other supporting components including compressed hydrogen cylinder, blower, solenoid valve, pressure regulator, water pump, heat exchanger and sensors. It was found that the vehicle performed satisfactorily over a 100-km drive on a plain route with the average speed about 18 km/h. Measurements also showed that the fuel cell system had an efficiency of over

30% at the power consumption required for vehicle cruise, which is higher than that of a typical Internal Combustion Engine.

The design, fabrication, and testing of an electric bicycle powered by a PEMFC has been reported by Hwang et al. [10]. The system comprises a 300 W PEMFC stack, MH hydrogen storage canisters, air pumps, solenoid valves, cooling fans, pressure and temperature sensors, and a microcontroller. The results showed that the system efficiency could reach up to 35%, and the ratio of travel distance to fuel consumption of the prototype electric bicycle was about 1.35 km g^{-1} H_2.

Table 1 – Typical operating characteristics of fuel cell powered vehicles. The records selected by *italic* correspond to the solutions where PEM fuel cells are used as on-board range extenders.

Application	Peak power [kW]	Bus voltage [V]	FC stack	Additional energy storage	Hydrogen storage[a]	Reference
Fuel cell powered electric bicycle	0.378	No DC/DC Up to 28	Air cooled PEMFC (0.3 kW)	Battery (start-up only)	MH (6.8 g H_2)	[10]
Mini-train	0.560	No DC/DC 12–24	Air cooled PEMFC (0.2 kW)	Lead-acid battery (18 V)	MH (50 g H_2)	[5]
Hybrid fuel cell wheelchair	0.678	28	Air cooled PEMFC (0.5 kW)	Li-ion battery (24 V, 14.6 Ah)	MH (21 g H_2)	[12]
Hydrogen fuel cell hybrid scooter	2.5	24	*Air cooled PEMFC (0.5 kW)*	*Lead-acid battery (24 V, 24 Ah)*	*MH (54 g H_2)*	*[13]*
Lightweight fuel cell vehicle	4.0	No DC/DC 38–56	Liquid cooled PEMFC (3.2 kW)	None	CGH2 (125 g H_2)	[9]
All-wheel-drive (AWD) vehicle	5.0	48	Air cooled PEMFC (2 × 1.5 kW)	Lead-acid battery (48 V, 45 Ah)	CGH2 (~0.29 kg H_2)	[4]
Light electric vehicle (LEV)	8.7	48	Liquid cooled PEMFC (6.0 kW)	Li-ion battery (48 V, 40 Ah)	MH (45.8 g H_2)	[3]
Light electric vehicle (golf cart)	10–12	48	*Air cooled PEMFC (1.2 kW)*	*Lead-acid battery (48 V, 242 Ah)*	*CGH2 (0.28 kg H_2)*	*This work*
Airport electric vehicle	16	80	Air cooled PEMFC (8.5 kW)	Lead-acid battery (84 V, 50 Ah)	CGH2 (1.34 kg H_2)	[14]
Hydrogen-electric hybrid urban vehicle	25	180	High temperature PEMFC (3.2 kW)	Li-ion battery (80 V, 60 Ah)	CGH2 (1.8 kg H_2)	[7]
EnerPac™ 48.1 fuel cell power pack for forklift	40	48	Air cooled PEMFC (8.5 kW)	Ni-MH battery + ultracapacitors (N/A)	CGH2 (0.97 kg H_2)	[15]
Fuel cell hybrid power source for electric forklift	50	80	Liquid cooled PEMFC (2 × 8.0 kW)	Lead-acid battery (80 V, 300 Ah) Ultracapacitors (80 F, 97.2 V)	MH (~0.36 kg H_2)	[16]
Fuel cell hybrid electric city bus	150	557–670	*Liquid cooled PEMFC (5.0 kW)*	*Na-$NiCl_2$ battery (278 V, 76 Ah)*	*CGH2 (9.6 kg H_2)*	*[17]*

a MH, metal hydride; CGH2, compressed hydrogen gas in cylinders.

Nadal and Barbir [11] described the design and performance of a prototype Zero Emission Electric Vehicle, powered primarily by three 21 kW air-breathing PEMFCs using gaseous hydrogen (w1 kg H_2) as fuel. The drive train system also included air compressor, solenoid valves, pressure regulators, water pump, water tank, heat exchangers, sensors, programmable controller, and voltage regulator. The battery system (10 batteries; 12 V, 1 kWh each) provided power to the vehicle during periods of peak load, such as vehicle acceleration or travelling at a high constant speed. The batteries also provided the power to initiate fuel cell start-up. The vehicle could travel several hundred kilometres solely on fuel cell power with satisfactory performance.

A novel hybrid fuel cell power train has been proposed by Yang et al. [12], for a wheelchair driven by rim motors. The power train consisted of a fuel cell, a DC/DC converter, and two secondary battery packs, and its energy management strategy was made to solve the problems of frequent charging of the batteries and large power fluctuations of the fuel cell system. The hybrid fuel cell power system was simulated, and the simulation results showed not only that the fuel cell was able to operate efficiently near a constant power, but also that the charging frequency of secondary batteries was reduced by about 98% compared to a series-hybrid fuel cell power train.

Typical specifications and operating performances of the fuel cell powered vehicles are summarised in Table 1; the records are sorted in ascending order of the maximum/peak system power (0.4-150 kW). Due to non-uniform power consumption during the operation of a FC-powered vehicle, the vehicular power systems usually have a hybrid layout with the PEMFC stack rated to the average power, while the surplus/peak power consumption by vehicle motors, as well as quick start-up of the system is provided by the batteries and/or the supercapacitors.

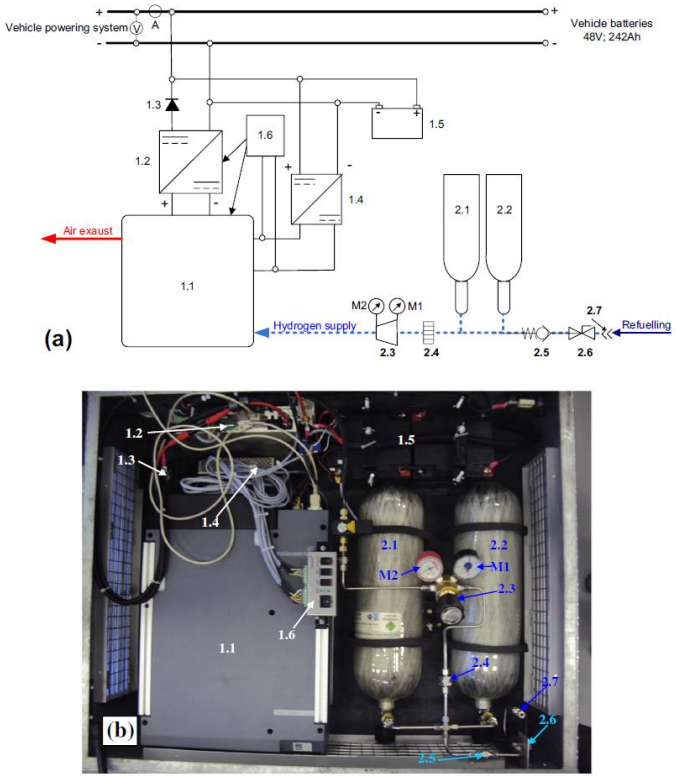

Fig. 1 – Schematics (a) and general view (b) of the on-board fuel cell power system: 1, Fuel cell power pack: 1.1, Nexa® 1200 fuel cell unit; 1.2, Nexa® DC1200 48 V DC/DC converter; 1.3, T70HFL20S02 reverse current diode; 1.4, 24 V step-down DC/DC converter; 1.5, 48 V/18 Ah battery pack; 1.6, Nexa DC1200 hybrid extension kit. 2, Hydrogen storage and supply system: 2.1, 2.2, Gas cylinders (6.8 L / 300 bar each); 2.3, Reducer: M1, high-pressure manometer; M2, low-pressure manometer; 2.4, Inline gas filter (0.5 μ); 2.5, Check valve; 2.6, Shut-off valve; 2.7, Refuelling connector.

Recently, special attention in the development of the FC-powered hybrid vehicles was paid to the solutions where PEMFCs are used as on-board range extenders. This approach allows to compromise system costs with its performances, by allowing the usage of lower power fuel cell stacks and smaller size vehicle batteries. The corresponding approach was realised by Shang and Pollet [13] who integrated a 500 W PEMFC into commercially available lead-acid battery electric scooter (2.5 kW in the peak power): the introduction of the fuel cell resulted in the range extension from 8 to 15 miles, increase of vehicle top speed and system energy efficiency. Andaloro et al. [17] developed a hybrid power train for an urban bus (150 kW in the peak power), by the integration of a 5 kW PEMFC. Cordner et al. [18] showed technical and economical feasibility of the integration of 1.2e13 kW PEMFCs as range extenders for racing electric cars with peak power 40e100 kW. It was also reported about activities in the development of fuel cell range extenders for airport EV's [19] and EV truck [20].

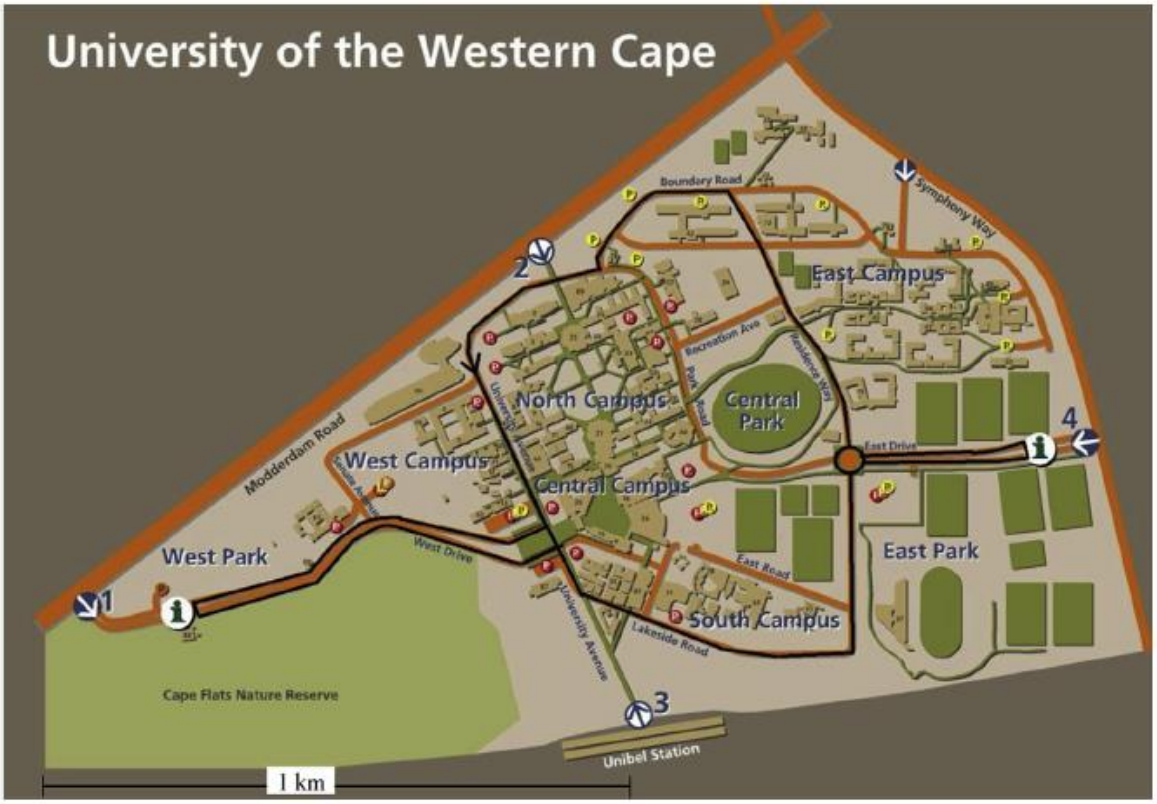

Fig. 2 – Vehicle test on the UWC campus (top) and the driving route (bottom).

The most important issue in the development of power systems for fuel cell hybrid vehicles is in the optimal sizing of the PEMFC stack (rated power) and batteries/supercapacitors (energy storage capacity and power density). The optimisation enables the design (i) to meet the end-user requirements for peak and average power, (ii) to meet space constraints, and (iii) to optimise capital and service costs.

Several attempts were undertaken to address the specified problem, mainly, by means of system modelling [6,8,12,16,17,21]. At the same time, quantitative information about the influence of introduction of a quite low-power fuel cell on the performance of battery electric vehicles is lacking and would be useful for the further modelling and optimisation activities.

In this work, an existing electric golf cart (5 kW in the nominal motor power) running on lead-acid batteries was hybridized with a 1.2 kW PEM fuel cell stack. A comparative study of the vehicle performances in the absence and presence of the fuel cell was carried out.

2. Materials and methods

2.1 System description

The hybrid system was built around a Melex Hi-Rise 4 seater vehicle (Melex Electrovehicles) used for everyday duties on the campus of the University of the Western Cape (UWC). The vehicle has a net weight of 760 kg (load up to 450 kg), overall dimensions of 3765 x 1290 x 2060 mm, and a wheel base of 2400 mm. The propulsion is provided by ZPJ5.0-100L-4 electric motor (5 kW/33 VAC) powered from eight US125xC lead-acid batteries connected in series (48 VDC, 242 Ah). The operation of the vehicle was provided by a Curtis1236 controller. The voltage (Fig. 1a; V) and current (A) sensors at the input of the vehicle power system allowed to monitor electric power withdrawn by the vehicle (>0) and returned to the battery (<0) during regenerative braking.

The life of a typical lead-acid battery is reduced by over-voltage, deep discharge (under-voltage) and high currents [22]. So the vehicle has its own built-in protection. The battery discharge indicator (BDI) reports 0 when a battery voltage of 37 V is reached and prevents operation of the vehicle. This strategy was not changed by the addition of the fuel cell as a “charger”. The fuel cell control strategy (see below) avoids over-voltage, and the battery life is actually expected to increase. The expectation is based on the assumption that the peak and average discharge current from the battery will be reduced, because part of the driving power comes from the fuel cell. Once the hydrogen supply to the fuel cell has been depleted, the battery will be operating without the “charger”, but this is not worse than the operation within the initial design.

The on-board fuel cell power system was assembled in the rear trunk of the vehicle (Fig. 1). It included a standard 1.2 kW PEMFC power system (1), [a]Heliocentris Energiesysteme GmbH, and hydrogen storage and supply system (2).

The main component of the power system (1) was a Nexa® 1200 fuel cell unit (1.1), with output voltage 20 to 36 VDC and maximum output current of 65 A (1200 W rated output power). The unit included an air cooled FCgen-1020ACS PEMFC stack (Ballard Power Systems; 36 cells) and the necessary peripheral components, including a controlled H_2 supply valve (input pressure 1e15 bar; flow rate up to 15 NL/min).

The fuel cell unit (1.1) was connected via a DC/DC converter (1.2; 48 VDC output) and reverse current diode (1.3) to the 48 VDC bus of the vehicle, in parallel. The step-down DC/DC converter (1.4) was used to supply the required voltage (24 VDC) for start-up of the fuel cell stack. Four 12 V 18 Ah lead-acid batteries connected in series (1.5) enabled additional storage of electric energy and provided power for system start-up. The system operation providing extended functionality was controlled by the Nexa® DC1200 Hybrid Extension Kit (1.6). The set-points for switching ON and OFF the FC system during running the vehicle corresponded to bus voltages of 50 and 52 V, respectively, or ±1 V as respect to the voltage (51 V) corresponding to 100% value of BDI set by the supplier of the vehicle.

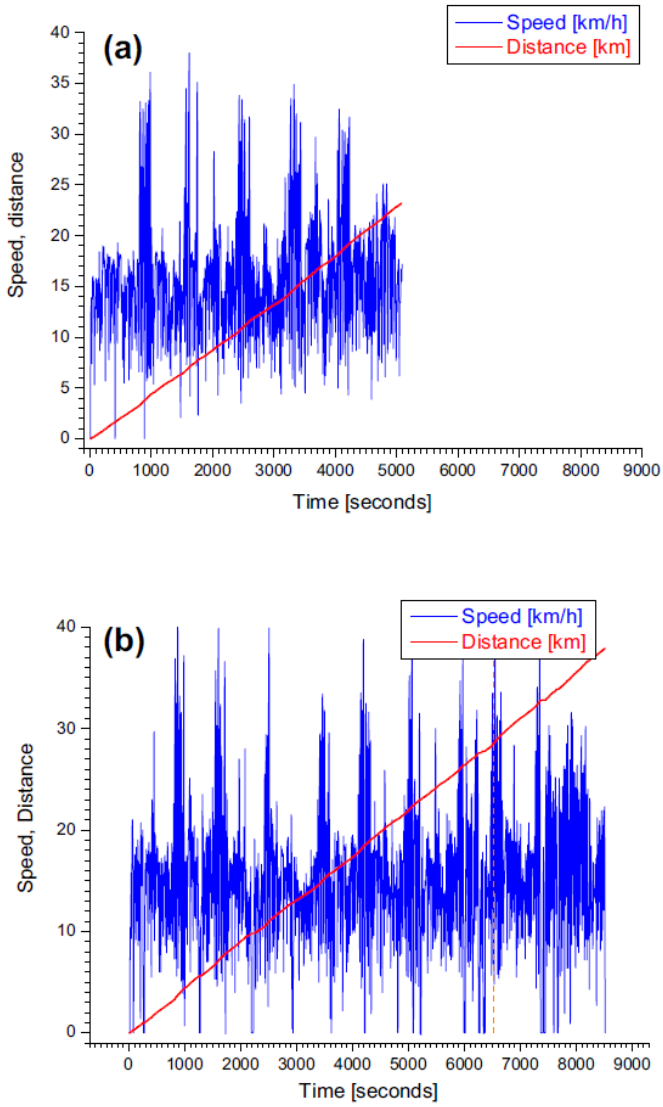

Fig. 3 – Logs of vehicle speed and driving distance taken during driving of the vehicle: (a) battery-powered, (b) hybrid (FC + battery)-powered. The vertical dashed line in (b) corresponds to the moment of shut-down of the FC stack (out of H_2).

The hydrogen storage and supply system (2) included two carbon-fibre reinforced fully wrapped aluminium-lined composite cylinders (2.1, 2.2; Shanghai Tianhai Dekun Composite Cylinders Co., Ltd), internal volume 6.8 L, operating pressure up to 300 bar. The system also included pressure reducer (2.3) equipped with high-pressure (M1) and low-pressure (M2) manometers, inline gas filter (2.4), check valve (2.5), shut-off valve (2.6), and refuelling connector (2.7). Prior to the tests using the fuel cell power system, it was refuelled with hydrogen (99.999%) from standard gas cylinders (Air Liquide, South Africa).

2.2. Testing procedure

The driving tests were performed at the UWC campus, on a flat route (see Fig. 2). The tests included (a) driving the golf cart in the battery-powered mode (FC stack

was off) and (b) driving in the hybrid (battery þ FC) powered mode. In both cases the batteries were first fully charged (BDI = 100%), and the route was the same. When driven in the hybrid mode, the hydrogen storage cylinders of the FC fuelling system were filled with H_2 to a pressure of 160 bar that corresponds to 1795 L H_2 STP, or 0.16 kg H_2 storage capacity. The tests were carried out at "forced" conditions when during driving the vehicle was periodically accelerated to 30e40 km/h followed by braking to 0e5 km/h. The driving in both battery- and hybrid-powering modes was carried out until discharge of the vehicle battery to 37 V that corresponds to the zero value of BDI set by the supplier of the vehicle. In the hybrid mode the fuel cell unit was switched off when nearly full consumption of hydrogen (residual H_2 pressure lower than 5 bar) was reached; so the amount of the consumed H_2 was about 155 g.

The details on the calculation of hydrogen consumption by the fuel cell unit (starting from hydrogen pressure in the system, or from the measured output power) are presented in the Supplementary information.

The data logging was carried out using the golf cart on-board data acquisition system, which uses a 1314 PC Programming Station environment ([a]Curtis Instruments; model 1314-4402, version 4.3.3). For logging the PEMFC parameters, the data acquisition software, Nexa® 1200 RC04 Control, supplied with the FC stack was used. The scan interval was set to 1 s.

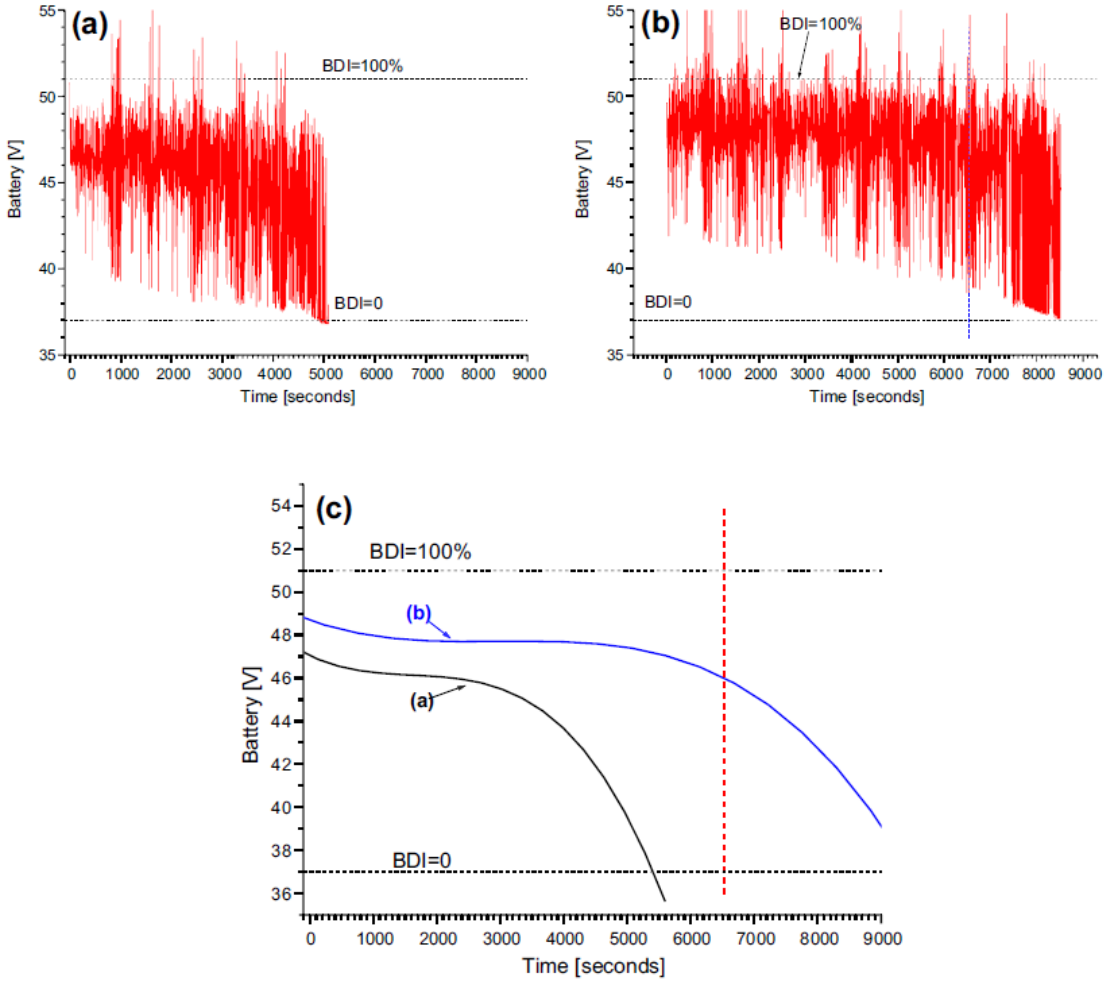

Fig. 4 – Logs of vehicle battery voltage taken during driving of the vehicle: (a) battery-powered, (b) hybrid (FC + battery)-powered, (c) comparison of the trend lines. The horizontal dashed lines correspond to the states of battery discharge indicator (BDI), and the vertical dashed lines – to the moment of shut-down of the FC stack (out of H_2).

Statistical analysis of the power patterns taken in the course of the data logging (the positive values correspond to withdrawn power, and the negative ones to the power returned for the battery recharge during the driving) was carried out with the help of Origin® software (OriginLab Corporation, version 6.1); the bin size was set to 300 W. Each dataset contained merged results (about 15,000 experimental points) of 2-3 driving tests performed in the same mode (battery or hybrid powered).

1. Results and discussion

Fig. 3 presents the logs of vehicle speed and running distance for driving the vehicle in battery-powered (a) and hybrid (battery þ FC)-powered (b) modes. It should be noted that in the latter mode more stable driving performances were observed, i.e. the vehicle could be accelerated easier and more frequently. More detailed consideration of this effect will be presented in Section 3.2.

A comparison of logs of vehicle battery voltage, in the battery-powered (a) and hybrid (battery þ FC)-powered (b) modes (Fig. 4) shows that in the latter mode the battery discharge takes place much slower, and the significant voltage drop is observed only after shutting the PEMFC stack down when hydrogen fuel is no longer available (c).

A comparison of power patterns recorded for powering modes (a) and (b) (Fig. 5) shows that in the hybrid mode (b), the withdrawn peak power (10e12 kW) was achieved more frequently than in the case of powering from battery only (a). The same tendency was observed for the returned peak power. The contribution of the power generated by PEMFC stack into the total power varies within 0e1.3 kW reaching the maximum during acceleration and dropping to 0-100 W during stops and driving with constant speed, when the absolute value of the total power is low.

The driving in battery-powering (a) and hybrid-powering (b) modes until the discharge of the battery (BDI = 0) was The observed value of the surplus energy consumed by the vehicle in hybrid mode (Withdrawn – Returned) was equal to 2.07 kWh that, taking into account the amount of the consumed H_2 fuel (0.155 kg) and the lower heating value of H_2 (33.333 kWh/characterised with similar loads and driving speeds on the same route (Fig. 2, Table 2). The operation in mode (b), even at incomplete H_2 fuel capacity (w55% of the maximum one), resulted in >63% extension of the driving range, as well as higher values of the energy withdrawn by the vehicle and the energy returned to the battery. As a result, the total energy consumed by the vehicle (withdrawn – returned) was 61% higher for the hybrid mode that corresponded well to the observed driving range extension. When the H_2 tanks are fully charged (P = 300 bar, 3116 L STP/0.28 kg H_2), the extension of the driving range is expected to increase to w110%.

Analysis of the data presented in Table 2 allows us to estimate the contribution of the fuel cell system into the energy balance of the vehicle in the hybrid-powering mode (b). The introduction of the fuel cell results in the increase of the energy withdrawn by the vehicle by (6.29 – 3.77) = 2.52 kWh. The energy returned to the battery was increased by (0.79 – 0.34) = 0.45 kWh. The observed value of the surplus energy consumed by the vehicle in hybrid mode (Withdrawn – Returned) was equal to 2.07 kWh that, taking into account the amount of the consumed H_2 fuel (0.155 kg) and the lower heating value of H_2 (33.333 kWh/kg), corresponds to a net fuel efficiency of the FC system of 40%. The estimated average H_2 consumption during fuel cell operation (travelling distance 28.6 km) was of 5.42 g/km.[1]

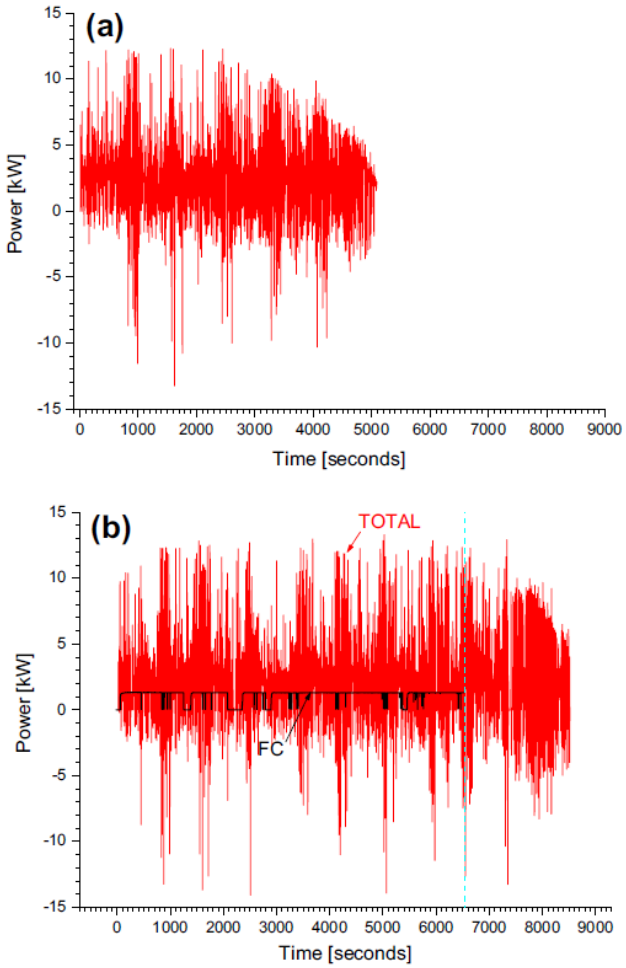

Fig. 5 – Typical power patterns taken during driving of the vehicle: (a) battery-powered, (b) hybrid (FC + battery)-powered. The vertical dashed line in (b) corresponds to the moment of shut-down of the FC stack (out of H_2).

Table 2 – Summary of the driving tests.

Parameter	(a) Battery only	(b) Battery + FC
Average speed [km/h]	16.1	15.8
Maximum distance [km]	23.2	37.9
Distance travelled during FC operation [km]	–	28.6
Time travelled [h]	1.44	2.40
Withdrawn energy [kWh]	3.77	6.29
Returned energy [kWh]	0.34	0.79
Total energy consumed [kWh]	3.43	5.50
Hydrogen fuel consumed [g]	–	133–155[a]

a The lower value was calculated from the FC power pattern; the higher one from the change of H_2 pressure in the fuel system.

From the data of Table 2 it can be calculated that the average power consumed by the vehicle varies from 2.29 (hybrid mode) to 2.38 kW (battery mode). Thus the increase of the fuel cell power to w2.5 kW, or about 50% of the nominal vehicle motor power, is expected to result in the possibility to avoid interruption of the vehicle operation for battery recharge which in this case could be provided only by the fuel cell during the driving. It will require the increase of the amount of the stored H_2 which should be enough to provide the operation of the higher power fuel cell during required driving period.

3.2. Statistic analysis of the power patterns

Fig. 6 presents the power distribution histograms taken from the power patterns when operating in battery-powered (a) and hybrid powered (b) modes. As it can be observed, the power distribution has the following features: (i) quite large number of counts at about zero power (standby mode of the vehicle), and (ii) rather smooth power distribution, which corresponds to the vehicle driving. The latter is characterised by two peaks where the first one corresponds to cruising and smooth acceleration (power > 0) and braking (power < 0). The second peak corresponds to the forced acceleration.

Driving in the hybrid-powering mode (Fig. 6b) is characterised by the wider first peak exhibiting higher percentage of the counts in both withdrawal (>0) of the power, and its return (<0) to the vehicle battery. Note that in this case the higher power return is caused not only by the regenerative braking, but also by the recharge of the battery from the fuel cell that corresponds well with the results of the driving tests (Table 2). The integrated histograms (Fig. 7) also show higher values of both withdrawn and returned power when operating in the hybrid (b) mode, as compared to the battery-powered (a) one. Also, the operation in the hybrid mode provides better forced acceleration as seen from the second peak (Fig. 6b), which is characterised by higher maximum and is narrower than that of the corresponding peak for the battery-powered mode (Fig. 6a).

Results of processing the power distribution data (excluding standby mode) are presented in Fig. 8 and Table 3. As it can be seen, in both cases the power patterns can be quite well fitted by two-peak Gaussian distribution function. From Table 3, it can be noted that the hybrid mode (b) can provide operation at the higher power, including both “soft driving” (average power corresponding to the centroid of the first peak about 1.8 kW, or w1.22 times higher than for the battery-powered mode (a)), and, also, “forced driving” (centroid at 7.8 kW that is 2.17 times higher than the operation in mode (a)). The latter feature explains better driving performances of the vehicle in the “forced” driving mode (including higher frequency and higher average values of the peak power) when using hybrid (FC þ battery) powering. In addition, the higher standard deviation of the fi st peak for the hybrid mode allows for the stable operation of the vehicle in a wider power range.

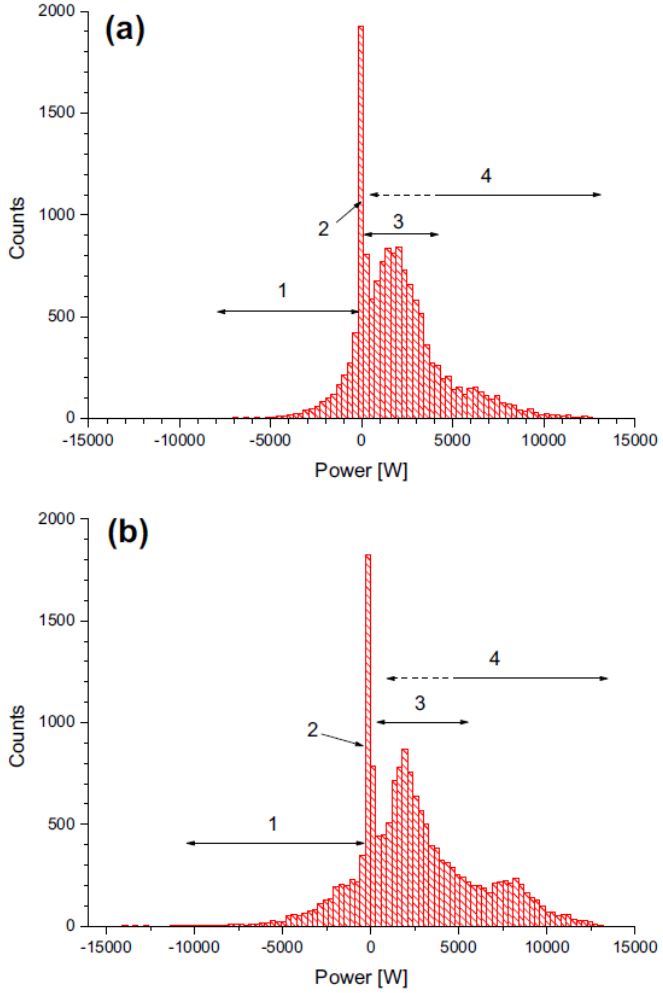

Fig. 6 – Power distribution histograms taken during driving of the vehicle: (a) battery-powered, (b) hybrid (FC + battery)-powered. The parts of the histograms correspond to regenerative braking (1), standby (2), cruise (3) and acceleration (4).

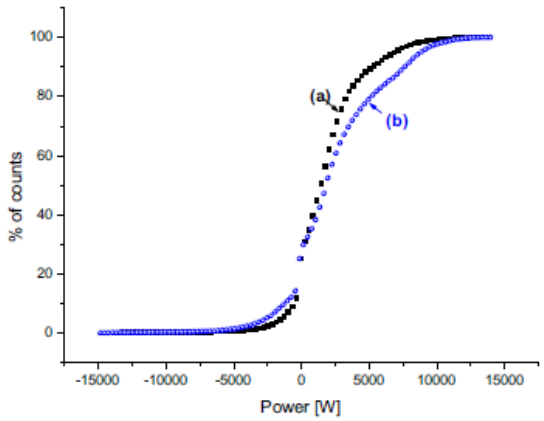

Fig. 7 – Integrated power distribution histograms taken during driving of the vehicle: (a) battery-powered, (b) hybrid (FC + battery)-powered.

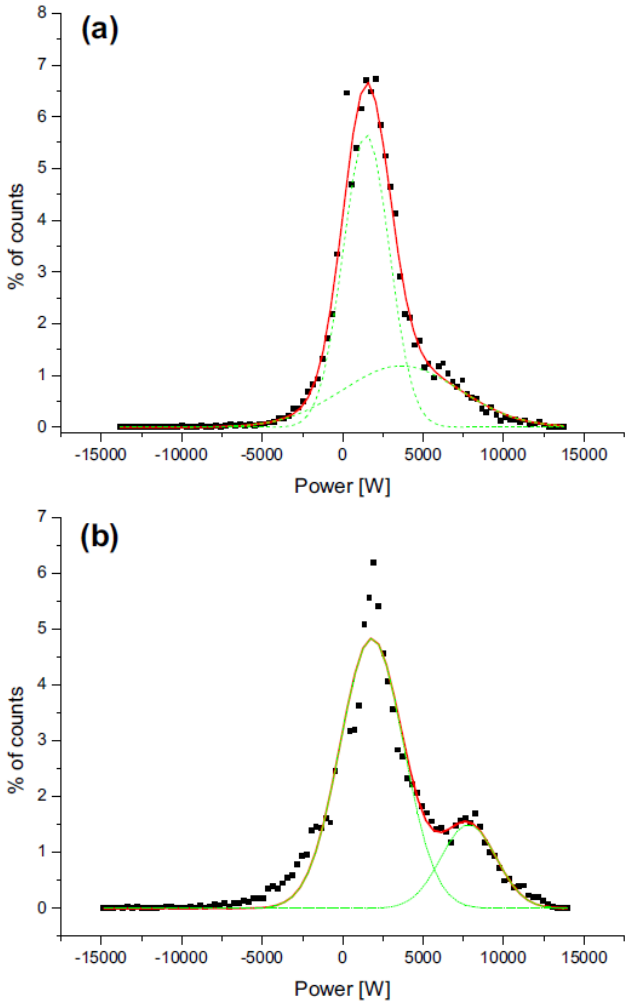

Fig. 8 – Gaussian fitting of the power distribution data (Fig. 6).

Table 3 – Fitting parameters of the power distribution data (Fig. 8).

Parameter	(a) Battery only		(b) Battery + FC	
	Value	Error	Value	Error
Centroid (1) [W]	1470	40	1800	70
Deviation (1) [W]	1440	60	1970	70
Amplitude (1) [%]	5.7	0.2	4.8	0.1
Centroid (2) [W]	3600	500	7800	200
Deviation (2) [W]	3600	300	1700	200
Amplitude (2) [%]	1.2	0.2	1.5	0.1
Pearson correlation coefficient, R^2	0.98288		0.95383	

4. Conclusions

Integration of 1.2 kW fuel cell system into light electric vehicle (5 kW nominal motor power) results in the extension of the vehicle driving range by 63e110%, when the amount of the stored H_2 fuel varies within 55e100% of the maximum capacity (0.28 kg H_2). The operation in the hybrid (battery þ fuel cell) powering mode results in more stable driving performance, as well as in the increase of the total energy both withdrawn from and returned to the vehicle battery during the driving.

On the basis of the test results, it is expected that the increase of the fuel cell power to w2.5 kW, or 50% of the nominal motor power, will enable to avoid the interruption of the vehicle operation for battery recharge which in this case could be provided only by the fuel cell during the driving.

Statistical analysis of the power patterns taken during driving in the battery and hybrid-powering modes showed that the latter provides stable operation in a wider power range, including higher frequency and higher average values of the peak power.

Acknowledgements

The work was funded by the Department of Science and Technology of South Africa via HySA Program, projects KP3-S02 and KP3-S03, and supported by Impala Platinum Holdings Limited (Implats), South Africa. The authors are also grateful to Melex Electrovehicles, South Africa, for providing the vehicle used in this study, as well as for the consultations regarding the features of the vehicle and its control system.

Appendix A. Supplementary information

Supplementary information related to this article can be found at http://dx.doi.org/10.1016/j.ijhydene.2013.06.072.

References

[1] Barbir F. PEM fuel cells: theory and practice. Burlington: Elsevier/Academic Press; 2005.
[2] Pollet BG, Staffell I, Shang JL. Current status of hybrid, battery and fuel cell electric vehicles: from electrochemistry to market prospects. Electrochim Acta 2012;84:235-9.
[3] Hwang JJ, Chang WR. Characteristic study on fuel cell/battery hybrid power system on a light electric vehicle. J Power Sources 2012;207:111-9.
[4] Barreras F, et al. Design and development of a multipurpose utility AWD electric vehicle with a hybrid powertrain based on PEM fuel cells and batteries. Int J Hydrogen Energy 2012;37:15367-79.
[5] Hsiao D-R, Huang B-W, Shih N-C. Development and dynamic characteristics of hybrid fuel cell-powered mini-train system. Int J Hydrogen Energy 2012;37:1058-66.
[6] Jiang Z, Gao L, Blackwelder MJ, Dougal RA. Design and experimental tests of control strategies for active hybrid fuel cell/battery power sources. J Power Sources 2004;130:163-71.
[7] Fisher P, Jostins J, Hilmansen S, Kendall K. Electronic integration of fuel cell and battery system in novel hybrid vehicle. J Power Sources 2012;220:114-21.
[8] Thounthong P, Raë l S, Davat B. Energy management of fuel cell/battery/supercapacitor hybrid power source for vehicle applications. J Power Sources 2009;193:376-85.
[9] Hwang JJ, Wang DY, Shih NC. Development of a lightweight fuel cell vehicle. J Power Sources 2005;141:108-15.
[10] Hwang JJ, Wang DY, Shih NC, Lai DY, Chen CK. Development of fuel-cell-powered electric bicycle. J Power Sources 2004;133:223-8.
[11] Nadal M, Barbir F. Development of a hybrid fuel/cell battery powered electric vehicle. Int J Hydrogen Energy 1996;21:497-505.
[12] Yang Y-P, Guan R-M, Huang Y-M. Hybrid fuel cell powertrain for a powered wheelchair driven by rim motors. J Power Sources 2012;212:192-204.
[13] Shang JL, Pollet BG. Hydrogen fuel cell hybrid scooter (HFCHS) with plug-in features on Birmingham campus. Int J Hydrogen Energy 2010;35:12709-15.
[14] Fontela P, et al. Airport electric vehicle powered by fuel cell. J Power Sources 2007;169:184-93.
[15] Infintium Fuel Cell Systems, Inc. EnerPac™ systems. Available from: http://ifcsglobal.com/products.html.
[16] Karanen TM, et al. Development of integrated fuel cell hybrid power source for electric forklift. J Power Sources 2011;196:9058-68.
[17] Andaloro L, Napoli G, Sergi F, Dispenza G, Antonucci V. Design of a hybrid electric fuel cell power train for an urban bus. Int J Hydrogen Energy 2013;38:7725-32.
[18] Cordner M, Matian M, Offer GJ, et al. Designing, building, testing and racing a low-cost fuel cell range extender for a motorsport application. J Power Sources 2010;195:7838e48.

[19] InnovaTek funding for fuel cell range extender in airport EV. Fuel Cells Bulletin June 2011:3e4.
[20] Integration of proton motor fuel cell range extender in EV truck. Fuel Cells Bulletin April 2012:2e3.
[21] Wishart J, Dong Z, Secanell M. Optimization of a PEM fuel cell system based on empirical data and a generalized electrochemical semi-empirical model. J Power Sources 2006;161:1041e55.
[22] Power Electronics and Photovoltaic Power Systems Laboratory, ECEN 4517/5517Lecture: lead-acid batteries. Department of Electrical and Computer Engineering, University of Colorado, http://ecee.colorado.edu/wecen4517/materials/Battery.pdf; Spring 2013.